Modelling the vulnerability of overhead lines against tree contacts for resilience assessment

E. Ciapessoni, D. Cirio, A. Pitto
Energy System Development Dept.
Ricerca sul Sistema Energetico - RSE S.p.A.
Milan, Italy
emanuele.ciapessoni@rse-web.it

G. Pirovano
T&D Dept.
Ricerca sul Sistema Energetico - RSE S.p.A.
Milan, Italy
giovanni.pirovano@rse-web.it

M. Sforna
Risk Management Unit
Terna S.p.A.
Milan, Italy
marino.sforna@terna.it

***Abstract*— The contact of overhead lines with vegetation represents a significant cause of failures, also as secondary effects of weather events such as strong wind, ice/snow accumulation. Thus, the management of the right of ways (ROW) of overhead lines is a key aspect to improve grid resilience. This paper proposes a probabilistic vulnerability model of overhead line failure due to inadvertent contact with vegetation, supporting the assessment of loss of load risk. The model can help TSOs to plan vegetation trimming campaigns and to alert operators in case of extreme weather events. Simulations on a realistic electric system demonstrate how the vulnerability model identifies the areas subject to tree fall. Moreover, its application within a resilience assessment methodology allows to relate the load interruption risk with both weather conditions (wind and snow loads) and deviations from ROW management standards.**

Keywords*— *resilience, tree contact, power systems, vulnerability

I. INTRODUCTION

Vegetation is a significant cause of overhead line (OHL) failures in High Voltage (HV) and Medium Voltage (MV) grids [1] and should be considered in resilience assessment analyses [2]. Tree-related failures may be caused by (1) vertical contact due to tree growth, possibly combined with increased line sag (responsible for only 2-15% of the total number of outages [3]), (2) fall of trees or branches on poles or conductors, (3) lateral contact of branches with conductors due to wind force, and possibly involve trees from outside the right of way (ROW) of the lines. These events typically occur during extreme weather events, whose frequency, extension, and severity is generally increasing [2]. Technical guidelines help operators determine the suitable ROW distance for each category of lines. As far as maintenance is concerned, adequate measures are to be deployed to keep the ROW clear from potential interferences due to vegetation or other objects. The availability of land cover data (CORINE database [4] in Europe) and of tree induced outage data may allow to characterize the tree contact threat and the relevant vulnerability of electric infrastructure. In [5] a proactive tool is proposed to anticipate the potential risks due to tree contacts, on the basis of weather forecasts, line vulnerability, tree cover and tree typologies derived from georeferenced datasets. However, such vulnerability models may be affected by inaccurate reporting from maintenance teams and by the low probability of the events. Moreover, as these models are based on statistics of past events, they do not provide information about the root causes of failures and on how the vulnerabilities and risks may change in future scenarios.

This paper proposes a physics-inspired analytical model of the line vulnerability to contact with trees. The model is probabilistic and has been integrated into the probabilistic risk and resilience assessment methodology described in [6]. The methodology thus enhanced is suitable to support operators by assessing the benefits of specific countermeasures (e.g. trimming campaigns) to increase power system resilience to tree-related threats.

The paper is organized as follows: Section II describes the analytical model of the OHL vulnerability to tree contact. Section III presents and discusses the application results on a case study referring to a realistic T&D (Transmission and Distribution) system. Conclusions are drawn in Section IV.

II. VULNERABILITY OF OHLS TO TREE CONTACTS

This section describes the probabilistic vulnerability model of MV and HV lines to tree contact.

A. Overall physical model

As reported in [1], the main factors affecting tree induced outages are: tree linear coverage density (no. of trees per km), clearance distance (horizontal distance between tree line and the closest phase conductor), tree species (trunk height, coniferous or broad leaf, maximum breaking strength), soil features (humidity, etc.), possible diseases of the trees, weather conditions (wind, snow, ice etc.), orography (terrain slope). The model of OHL vulnerability to tree contacts considers the interaction between the geometry and the operating condition of the line (e.g. support height, span length, flowing current), environmental factors (e.g. air temperature, wind speed, precipitation rate), tree characteristics (e.g. its weight) and the spatial relationships between the tree and the line.

Let us consider a line (see Fig. 1a) surrounded by trees with a linear coverage density δ_{out} outside the ROW and possibly a density δ_{in} inside the ROW in case maintenance was not carried out properly. Let us define P_f the probability of event F, i.e. failure of a line span due to the contact of a tree. Event F can be caused by the lateral contact (event C) due to the tree fall or the lateral swing of the conductor onto a tree branch, and/or to a vertical contact (event V):

$$F = C \cup V \tag{1}$$

Considering that trees can be inside (event I) and/or outside (event O) the ROW leads to (2) and then to (3).

$$F = (C \cup V) \cap (O \cup I) \tag{2}$$

$$F = (C \cap O) \cup (C \cap I) \cup (V \cap O) \cup (V \cap I) \tag{3}$$

Events $(C \cap I)$ and $(V \cap O)$ can be assumed as empty ($\varnothing$) because negligible harm can be provoked by the fall of trees inside the ROW or by the vertical contact of trees outside the ROW. Thus equation (3) can be simplified as (4).

$$F = (C \cap O) \cup (V \cap I) \tag{4}$$

where $(C \cap O)$ and $(V \cap I)$ respectively represent the independent events that a tree inside the ROW has a vertical

contact with a phase conductor, and that a tree outside the ROW has a lateral contact with the phase conductor. Thus the probability of F i.e. P_f can be written as:

$$P_f = 1 - [(1 - \Pr(C \cap O)) \times (1 - \Pr(V \cap I))] \quad (5)$$

B. Model of vertical contact

The growth of the trees inside the ROW can make the clearing distance between the lowest point of the line conductors and the tree become lower than the minimum admissible value depending on the voltage level. The lowest point of the line conductor depends on the flowing current and on environmental conditions. The exploitation of the heat balance equation of the conductor [7] allows to derive a probability distribution of the line sag. Each tree height is characterized by a Gaussian probabilistic model whose CDF_{ht_inROW} is centered on the expected height depending on the height at time t_1 (latest trimming time) and variance increases proportionally from t_1 [8]. The vulnerability of the line to vertical contacts is assessed by the following steps:

1) Apply forecast ambient conditions (with uncertainties) to the heat balance equation of the conductors
2) Derive the probability distribution of line sag pdf_{sag}
3) Compare the tree height against the height of the lowest point of the line. In particular, check if the sum of the stochastic variables *sag* and tree height h_{t_inROW} is higher than quantity $TS = HS - br \cdot \sin(slope)$:

$$h_{t\_inROW} + sag > TS \quad (6)$$

where *br* is the width of the lowest cross-arm and *HS* is the height of the corresponding connection point of the conductors. Term $br \cdot \sin(slope)$ represents the effect of slope and assumes that tree inside the ROW grow on the uphill side of ROW.

If condition (6) holds true, the tree causes the line to contact the ground due to vertical contact.

The ambient variables considered in step 1 are the ambient temperature, the wind speed and direction, the possible precipitation rate and the solar irradiation. The probability distribution of the sum y of the two variables *sag* and h_{t_inROW} is evaluated by applying the convolution between the two densities pdf_{sag} and pdf_{ht_inROW} as in (7):

$$S(y) = (pdf_{sag} * pdf_{ht\_inROW}) = \int_0^y pdf_{sag}(y-\xi) \cdot pdf_{ht\_inROW}(\xi) d\xi \quad (7)$$

Condition (6) can be expressed with the integral $\int_{TS}^{\infty} S(y)dy$.

Term $\Pr(V \cap I)$ representing the probability that any of the trees in the ROW of one line span with length L has a vertical contact is the probability of the OR of all the potential contacts on the basis of the number of trees inside the ROW and it can be formulated as in (8):

$$\Pr(V \cap I) = 1 - (1 - \Theta)^{\delta_{in} L} \quad (8)$$

where

$$\Theta = \int_{TS}^{\infty} S(y) \cdot dy \quad (9)$$

δ_{in} is the linear coverage density of trees inside the ROW (in number of trees/km) and Θ is the probability that a single tree has a vertical contact with the conductor.

C. Model of lateral contact due to tree fall

Term $\Pr(C \cap O)$ represents the probability that a tree (or part of it) from outside the ROW comes into contact with the phase conductor causing line failure, i.e. it represents the failure probability of the line due to the lateral contact of any of the trees along the ROW of the line span. The diversity of possible situations (fall of the whole tree, rupture of branches, etc.) imposes to set some assumptions:

- the focus is on the following phenomena:
  - the fall of the whole tree (due the stem breakage or the failure of the root-soil anchoring system),
  - the lateral swinging of conductors
- the soil is characterized only in terms of its slope
- the wind which tends to overturn the tree towards the line also causes the conductor on the opposite side of the line to approach to the boundary of ROW. In order to simulate the tree fall mechanism, the most pessimistic position of the conductor during its swinging i.e. the vertical position of the line sag, is assumed (condition at zero wind). The dynamics of the conductor oscillations which can bring temporarily the conductor closer to the ROW boundary is neglected.

The probability of failure due to the fall of trees along the ROW depends on many factors:

- the *features of tree species* (height, weight, and mechanical properties like the overturning limit moment, maximum breaking load of the branches),
- the *soil features* (slope, humidity),
- the *weather conditions* (wind, wet snow load).

Fig. 1a shows the force diagram.

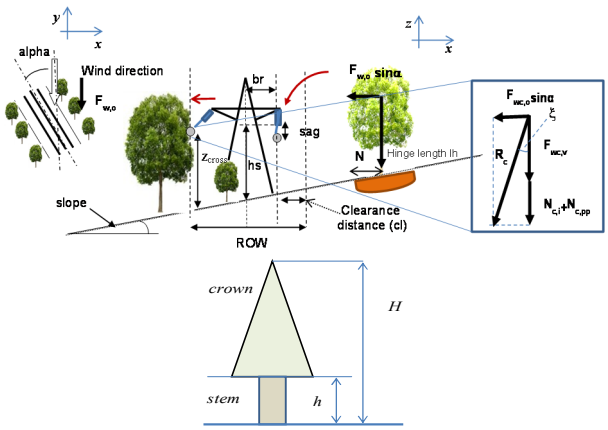

Fig. 1. Interaction environment- line: (a) Diagram of the forces acting on the {line, environment} system, (b) tree structure with crown and stem [14]

The resulting forces on the tree and on the conductor include both horizontal components (subscript "o") of wind induced forces F_w and $F_{w,c}$ and vertical components N and N_c which may include also possible vertical components (subscript "v") of F_w and $F_{w,c}$. Starting from a probability distribution CDF_{ht_outROW} defined for the height of a single tree outside the ROW, the failure probability due to lateral fall corresponds to the probability that

(*i*) the overturning moment $M_{overturning}$ due to combined wind and wet snow action on the tree exceeds the limit moment for overturning M_{R_ov} or the limit moment for stem breakage $M_{R\_breakage}$, and

(*ii*) the tree height is higher than distance $(h_c^2 + la^2 + cl^2)^{0.5}$ where h_c is the height of the lowest point of the phase conductor from the terrain, *cl* is the clearance distance (see Fig. 1a) and *la* is the distance along the direction of the line.

Thus the two conditions in (10) must be met.

$$M_{overturning} > M_{R\_ov} \text{ OR } M_{overturning} > M_{R\_breakage}$$
$$\text{AND}$$
$$h_{t\_outROW} - (h_c^2 + la^2 + cl^2)^{0.5} > 0 \quad (10)$$

where h_c, cl and $M_{overturning}$ depend on weather conditions (specifically, the k hour ahead forecasts for operational planning studies, the conditions associated with a specific return time for long term planning analyses). M_{R_ov} and $M_{R\_breakage}$ are set as Gaussian distributions with an expected value representing an average behavior for each member of the tree species and an uncertainty due to the various conditions (such as weather hazards, tree age, diseases etc.) affecting it over the years.

The tree [9]-[15] is characterized in terms of height h (m), density δ (kg/m^3), Young's modulus E (Pa), Modulus Of Rupture MOR (Pa), root rotational stiffness k (kN·m/rad), width of root–soil plate l_T (m). The tree width dbh in cm is correlated to the tree height [10] as in (11).

$$dbh = a_0 + a_1 \times h \quad (11)$$

Crown diameter c can be derived from dbh using (12).

$$c = 2 \cdot (b_0 + b_1 \cdot dbh) \quad (12)$$

where parameters a_0, a_1, b_0 and b_1 depend on the type of tree. The root-soil system [11][12] acts as an anchorage for the tree and applies a resistive moment to avoid the overturning of the tree.

The wind force depends on the wind speed profile above the ground. The model assumes the wind force and the normal force are applied to the center of gravity of the tree. Modeling the tree as a cone (the tree crown) superimposed to a cylinder (the stem, see Fig. 1b for coniferous species), the height of the center of gravity z_g is given in [10] by $(H+2h)/3$ where H is the total height of the tree and h is the stem base height.

The intensity of the wind-induced force is given by the dynamic pressure of the wind multiplied by the combined area of the tree crown and stem as in (13).

$$F_w = 0.5 \times C_d \times G \times \rho \times A_t \times w^2 \quad (13)$$

$A_t = A_{stem} + A_{crown} = dbh \times h + S \times c \times (H - h) \times 0.5$ where $S = \frac{10}{w} - 0.1$ takes into account the streamlining of wind through crown branches: this relationship holds valid for wind speeds w between 10 and 20 m/s. G is the gust factor which takes into account the distance of the tree from the edge of the forest and the spacing among trees, and is given in [13]. C_d is the drag coefficient and it is given by $1.77\, w^{-0.911}$ [13]; w is the wind speed computed at center of gravity height z_g, following the wind speed profile curve with a reference speed w_{ref} at reference height z_{ref} and terrain rugosity z_0

$$w = w_{ref} \times \ln\left(\frac{z_g}{z_0}\right) \Big/ \ln\left(\frac{z_{ref}}{z_0}\right) \quad (14)$$

The wind-induced lateral force determines a horizontal displacement of the tree associated to the bending of the stem due to its elasticity, and the rotation of the root system according to the root stiffness [9].

The first contribution to displacement is computed in (15) where E is the Young's modulus of the tree and I is the inertia moment defined as $\pi d^4/64$ where d is the stem width at the height of gravity center (assumed equal to dbh) [9]:

$$X1 = F_{w,o} \times z_g^2 \times H \times (3 - z_g / H - 3 \times (1 - z_g)/H) / 6EI \quad (15)$$

The second term superimposed to $X1$ is due to the rotation of the root system caused by the bending moment of the force $F_{w,o}$ as in (16).

$$X2 = z_g \times \frac{M_{bend}}{k} \quad (16)$$

where $M_{bend} = F_{w,o} \times z_g$

The total displacement is given by $X = X1 + X2$.

The *vertical force* is due to the tree's own weight, to the potential snow load on top of it, and to a potential vertical component $F_{w,v}$ of wind induced force:

$$N = N_{tree} + N_{snow} + F_{w,v} \quad (17)$$

Tree's weight N_{tree} includes the stem weight and the crown weight which is estimated as a fraction of the stem weight (ranging from 0.44 to 1 for most trees) [10]. The total *overturning moment* is given by (18).

$$M_{overturning} = F_{w,o} \times \left[z_g \times \cos\varphi + lh \times \sin(slope + \varphi)\right] + \\ + N \times \left[X - lh \times \cos(slope + \varphi)\right] \quad (18)$$

where lh is the hinge length which corresponds to half of the width of the root-soil plate l_T.

For the breakage or the overturning of the tree, at least one of the following conditions must be verified from (10):

$$M_{overturning} > M_{R\_ov} \quad (19a)$$
$$M_{overturning} > M_{R\_breakage} \quad (19b)$$

The *limit moments* are M_{R_ov} and $M_{R\_breakage}$. The former is calculated according to [13] as in (20).

$$M_{R\_ov} = g \times \frac{R_{mass} \times R_{depth}}{f_{SW}} \quad (20)$$

where R_{mass} is the mass of root-soil plate, R_{depth} is the depth of the root-soil plate, and f_{SW} is the fraction of the total resistive root moment due to the root-soil system mass, normally ranging between 0.2-0.3. Limit moment $M_{R\_breakage}$ is a function of MOR (Modulus of Rupture, in Pa) as reported in (21) [13].

$$M_{R\_breakage} = \pi \times MOR \times dbh^3 / 32 \quad (21)$$

When the overturning of the tree has occurred, it is assumed that the soil-root system is no longer connected to the ground, thus the resistive moment of this system becomes null. Accordingly, the force scheme changes and the overturned tree can be considered as an object laying on an inclined plane. This means that the slope reacts to the component of force N which is normal to the inclined plane, while the components of wind induced force $F_{w,o}$ and N parallel to the plane act on the tree determining the trajectory of the tree during the fall. This allows to determine the potential interception with the line. Distance $D_2 = (h_c^2 + la^2 + cl^2)^{0.5}$ must take into account the sag of the line (computed in the previous subsection) but also the available clearance distance cl, see (22).

$$D_2 = \sqrt{\left(ROW/2 - br\right)^2 \cdot \left(1 + \left(\frac{1}{\tan\Phi}\right)^2\right) + \left(HS - sag \pm ROW \cdot \sin(slope)/2\right)^2} \quad (22)$$

where br is the cross-arm width supporting the conductor, while sag is the conductor sag affected by the ambient conditions and described by pdf_{sag} derived in subsection II.B, and the sign "+" ("-") is used in case the wind is oriented in downhill (uphill) direction. Angle Φ is the

arctangent of the ratio between the two components of the resulting force projected on the slope plane, as in (23).

$$\Phi = \arctan\left(\frac{N\sin(slope) + F_{w,o}\sin\alpha\cos(slope)}{F_{w,o}\cos\alpha}\right) \quad (23)$$

The probability P_{Ctree} that a single tree falls and intercepts the line is given by the probability of the AND of the two conditions in (10). A Monte Carlo sampling technique is used to estimate the two terms of (24).

$$P_{Ctree} = \left[1 - \Pr(M_{overturning} - M_{R\_ov} > 0)\cdot\Pr(M_{overturning} - M_{R\_breakage} > 0)\right]\times \quad (24)$$
$$\times\Pr(h_{t\_outROW} - (h_c^2 + \mathrm{la}^2 + cl^2)^{0.5} > 0)$$

Term $\Pr(C \cap O)$ represents the probability that a tree outside the ROW and along line span with length L falls and intercepts the line. This term also accounts for relevant linear coverage density of the trees outside the ROW, δ_{out}, as in (25):

$$\Pr(C \cap O) = 1 - (1 - P_{Ctree})^{\delta_{out}L} \quad (25)$$

Adequate derating factors are derived from [10] for overturning limit moment and hinge length, and applied to the model, in order to assess the effects of water content on the root-soil plate.

D. Model of lateral contact due to line conductor swing

Fig. 1a reports the configuration and the force scheme to describe the lateral contact of the conductor with a tree close to the ROW boundary. The resulting force R_c acting on the conductor is composed by:

- a vertical component given by the own weight of the conductor ($N_{c,pp}$), by the ice/wet snow load ($N_{c,i}$), and by the vertical component $F_{wc,v}$ of the wind induced force
- a horizontal component due to wind on conductor $F_{wc,o}$

The wind induced force F_{wc} is computed using the formula in EN 50341-1 standard [16]. The line sag will be inclined by an angle ξ with respect to the vertical axis where ξ is given by (26).

$$\xi = \arctan\left(\frac{F_{wc,o}\sin\alpha}{F_{wc,v} + N_{c,i} + N_{c,pp}}\right) \quad (26)$$

The conditions for the lateral contact are two-fold:

- the inclined sag must satisfy (27);

$$sag\times\sin\xi \geq \frac{ROW}{2} - br \quad (27)$$

- the tree at the ROW boundary must be higher than the minimum point of crossing z_{cross} of the sag through the ROW boundary, see (28), accounting for the slope and the wind direction:

$$h_{t\_outROW} \pm ROW/2\cdot\sin(slope) \geq HS - \sqrt{(Q_{sag}^{0.99})^2 - (ROW/2 - br)^2} \quad (28)$$
$$\text{if } Q_{sag}^{0.99} \geq ROW/2 - br$$

where $Q_{sag}^{0.99}$ is the 99th quantile of the sag of the line. The sign "+" ("-") is used in case the wind blows in the uphill (downhill) direction. The line sag and angle ξ are computed as stochastic output of the mechanistic model of the heat balance of the bare conductors fed by stochastic inputs such as ambient temperature and wind speed, in the same way as in subsection II.B. The probability of failure due to lateral contact is given by the product of the probability of occurrence of the two abovementioned conditions i.e. equation (29) holds valid.

$$\Pr\left(sag\times\sin\xi \geq \frac{ROW}{2} - br\right)\times$$
$$\Pr\left(h_{t\_outROW} \pm ROW/2\cdot\sin(slope) \geq HS - \sqrt{(Q_{sag}^{0.99})^2 - (ROW/2 - br)^2}\right) \quad (29)$$

In case $Q_{sag}^{0.99} < ROW/2 - br$ the relevant probability is zero because under this condition the lateral swing of the conductor is limited and cannot reach the ROW boundary. Thus, the final probability of failure of a line span due to vertical contact and/or lateral fall of the trees inside and outside the ROW is given by (30).

$$P_f = 1 - \left[\left(1 - \int_{TS}^{\infty} S(y)dy\right)^{\delta_{in}L}\times\ldots\right.$$
$$\left.\ldots\times\left\{\begin{array}{l}\left(1 - \Pr(M_{overturning} - M_{\lim} > 0)\times\right.\\ \left.\Pr(h_{t\_outROW} - (h_c^2 + \mathrm{la}^2 + cl^2)^{0.5} > 0)\right)\times\\ \left[1 - \Pr\left(sag\times\sin\xi \geq \frac{ROW}{2} - br\right)\right.\\ \left.\times\Pr\left(\begin{array}{l}h_{t\_outROW} \pm ROW/2\cdot\sin(slope) \geq \ldots\\ \ldots \geq HS - \sqrt{(Q_{sag}^{0.99})^2 - (ROW/2 - br)^2}\end{array}\right)\right]\end{array}\right\}^{\delta_{out}L}\right] \quad (30)$$

The failure probability $P_{f,TOT}$ of the whole line composed by N_s spans each with a failure probability $P_{f,i}$ is given by (31).

$$P_{f,TOT} = 1 - \prod_{i=1}^{N_s}(1 - P_{f,i}) \quad (31)$$

E. Data requirements

The role of the data is essential to properly characterize the interaction between the lines and the surrounding environment, thus the vulnerability models soundness. To this aim, the vulnerability model herein developed exploits both national and international design standards for lines [17] as well as publicly available databases in order to retrieve realistic information about the slope of the terrain, the forecasts of weather conditions, and the tree coverage. The slope of the terrain is derived by geometric interpolation from the level curves of the terrain. The forecasts of weather conditions are provided from numerical weather prediction models and the tree coverage maps are extracted from CORINE database [4].

III. Study Case

The vulnerability model, integrated into a risk-based resilience assessment tool [6], was applied to a real world study case. The vulnerability models of MV and HV lines are parametrized using standard values and design criteria: specific line parameters (geometry, mechanical resistance etc.) and criteria can also be used to customize the vulnerability models on the basis of detailed information if available. The resilience assessment tool combines threat and vulnerability probabilistic models, getting the list of the most critical lines (i.e. the ones with highest failure probability) and consequently the list of the most risky (also multiple common mode and dependent) contingencies involving these lines. The adopted risk indicator is the expected loss of load (LOL) [6].

A. Test system

The test system integrates two MV feeders involved in the Deval DSO "Smart Grid" project, promoted by the Italian Regulatory Authority ARERA [18], and a portion of the surrounding HV/EHV transmission grid in Aosta Valley, Italy (see Fig. 2.) around the HV/MV primary substation of

Villeneuve, particularly critical as it provides energy to a large area (770 km^2). The MV/HV grid model, derived from Deval [18], [19], and Terna [20] public references, includes 92 MV electrical nodes (of which 60 are MV/LV substation nodes), 8 EHV (220 kV) nodes, 10 HV (132 kV) nodes, 20 HV OHLs and 3 EHV/HV transformers.

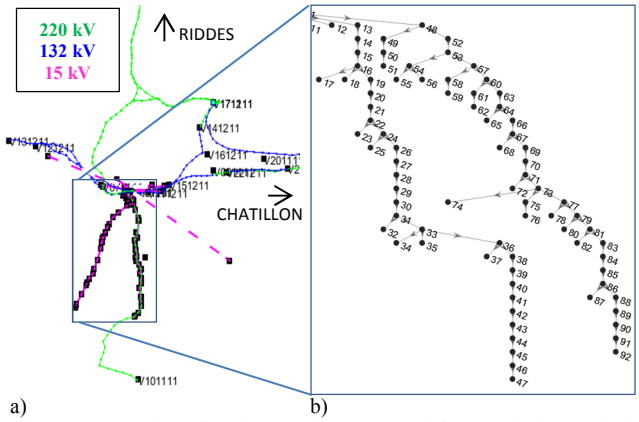

a) b)

Fig. 2. Integrated MV/HV/EHV grid: (a) map of the MV feeders and of the surrounding HV grid, (b) one-line diagram of the two feeders

The forecast weather conditions for the base case refer to a severe wet snow storm in the North of Italy occurred in February 2015, the level curves of the terrain are extracted from the website at [19] and the "level-3" tree coverage information was retrieved from CORINE database [4]. The wind load assumed for the simulation is the maximum value forecasted for the specific geographical location in the 72 hours ahead, while the wet snow load is computed considering the forecasted hours with the simultaneous presence of a not null precipitation rate in the temperatures range (-0.5/+1.5 °C). The region under study was marginally struck by the Feb 2015 event, and the highest values for the forecasted wind speeds (mean value on a 4×4 km area) are around 45 km/h. Locally wind gusts are characterized by wind speed values much higher (also 2-3 times higher) than the mean value forecasted by Numerical Weather Forecast, which is taken into account in the model. The expected values of the parameters characterizing the trees (mainly larches) are reported in TABLE I.

TABLE I - PARAMETERS OF TREE FORESTS IN THE STUDIED REGION

Parameter	Measurement unit	Value
Linear coverage density inside ROW δ_{in}	Nr of trees/km	10
Linear coverage density outside ROW δ_{out}	Nr of trees/km	50
Tree height outside ROW	m	20
Tree weight outside ROW	kg/m^3	800
Young's Modulus	MPa	12 10^6
Modulus of Rupture	MPa	50 10^6
Rotational stiffness of roots	kN m/rad	10^4

For larches, the following values for the parameters in equations (21) are adopted: a_0 = 0, a_1= 40/28, b_0= 0.9488, b_1= 0.0356. The bracing widths and the support heights for HV (MV) line towers are respectively 6 (0.8) m and 30 (12) m. Both copper and ACSR standard conductors are adopted for MV lines, while ACSR standard conductors are used in HV and EHV lines.

The ROW value in the base case is calculated according to the function in (32) which represents the best second order polynomial fit reproducing the typical ROW widths adopted by grid operators [21] as a function of voltage level.

$$ROW = (-10^{-4} \cdot V_{nom}^2 + 0.1425 \cdot V_{nom} + 12.163) \qquad (32)$$

where ROW is the right of way width in m, V_{nom} is the nominal line voltage in kV. TABLE II reports the list of simulation cases.

TABLE II - SUMMARY OF THE SIMULATIONS

ID	Description	Goal
1	Base case scenario	Validate the model capability in detecting critical areas
2	Weather conditions are worsened, by applying a 3 multiplying factor to wind speed profiles	Quantify the effect of weather conditions on system resilience
3	ROW widths are enlarged by 30%	Quantify the effect of a different ROW management policy on system resilience
4	Expected height of trees outside ROW is brought from 20 m to 10 m	

B. Base case analysis

The application of the base case scenario to the grid model identifies 7 critical lines i.e. the lines more prone to fail due to tree contact (see TABLE III).

TABLE III – LIST OF CRITICAL LINES WITH THEIR CONDITIONAL FAILURE PROBABILITIES, BASE CASE AND 30% ROW ENLARGEMENT

Base case		130% ROW	
Component ID	Cond. Fail. probability	Component ID	Cond. fail. probability
D853311 - D863311	8.05×10^{-1}	D853311 - D863311	4.34×10^{-1}
D863311 - D883311	6.69×10^{-1}	D863311 - D883311	3.88×10^{-1}
D903311 - D913311	5.47×10^{-1}	D903311 - D913311	3.26×10^{-1}
D883311 - D893311	4.58×10^{-1}	D883311 - D893311	2.33×10^{-1}
D893311 - D903311	1.93×10^{-1}	D893311 - D903311	1.60×10^{-1}
D843311 - D853311	1.85×10^{-1}	D843311 - D853311	8.50×10^{-2}
D833311 - D843311	1.19×10^{-1}		

All the involved lines are MV lines which are clearly more affected than HV lines by tree contacts due to their smaller size. These MV lines all belong to the "Val Savarenche" feeder: the risk of tree fall in this zone (around nodes #80 and 86) is confirmed by the DEVAL resilience plan [22] which in fact proposes the construction of an underground cable as a counterfeed among nodes #26, 72, 80 and 86 to improve the resilience of the area. This good matching obtained using only standard design criteria for the lines and public datasets confirms the relatively low sensitivity of the model with respect to the chosen parameters provided that reasonable ranges are assumed for the parameters themselves. After that, the second stage consists in identifying the most risky contingencies involving these critical lines. They consist in N-1 branch outages, N-k common mode branch outages, and N-k busbar dependent contingencies which lead to a total loss of load risk indicator equal to 0.508 expected lost MW. Fig. 3a reports the absolute contribution to the risk of load disruption for each contingency category.

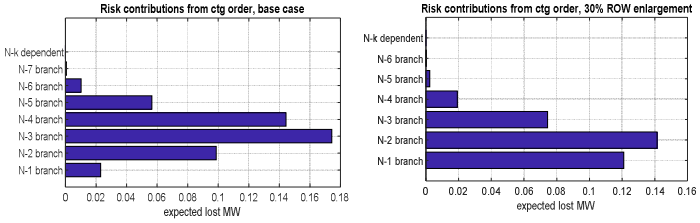

(a) (b)

Fig. 3. Results of risk based resilience assessment: histogram of the contributions of each contingency category to the overall LOL risk in expected lost MW (a) in the base case, and (b) in case of 130% ROW.

The largest contributions to the overall loss of load risk come from multiple common mode branch contingencies

which have also the largest median impact indicator (around 0.6 lost MW). Relatively low-order contingencies (such as N-2) can have significant median LOL impacts due to the absence of a counterfeed which can take over the last part of the Val Savarenche feeder. This demonstrates the need for the underground cable explained in [22].

C. *Quantifying the effect of weather condition severity*

In this scenario, the weather conditions of the base case are increased to the same maximum values of wind speeds (up to 100 km/h) forecasted in the areas -Lombardy and Emilia Romagna regions- affected by the storm in Feb 2015. These conditions may favor the overturning of trees especially due to the high wind gust speeds combined with increased weight of the tree due to snow accumulation. The number of critical lines increases from 7 in the base case to 17 lines of which 4 belong to HV grid and 13 to the MV grid: the highest median values for the LOL impacts, which are associated with N-k common mode branch contingencies with k=15, 16 and 17, are equal to 11.1 MW. The interesting aspect is that the HV lines indicated as critical are characterized by a significant wet snow load (up to 18 kg/m) which cause sags up to 13 m thus favouring the interception between falling trees and the line in case of strong winds.

D. *Quantifying the effect of the ROW maintenance policies*

This scenario considers an enlargement of the ROW width by 30% with respect to the values from (32). Table III shows that the number of critical lines reduces from 7 to 6 and the failure probabilities of the remaining critical lines decrease by a relatively low amount. This is due to the fact that larches have a height up to 30 m and generally the ROW assigned to MV lines is relatively small (around 15-20 m). Again the contingencies involving the critical components are identified and simulated: Fig. 3b) reports the contribution of each contingency category to the total risk of load disruption. In this case the total LOL risk passes from 0.508 to 0.358 expected lost MW's (30% reduction), of which the largest contributions are due to N-k common mode branch outages. The conclusion is that a 30% enlargement does not represent a very effective measure if the trees outside the ROW are not properly trimmed.

To demonstrate the effect of trimming, it is assumed that the trimming policy changes in the utility: the ROW is kept unchanged as in the base case but the expected height for trees just outside the ROW is kept at 10 m by applying a more frequent trimming procedure. Setting an expected tree height of 10 m with the same uncertainty as in the base case leads to the absence of critical lines.

IV. Conclusions

This paper has presented an innovative vulnerability model of MV and HV OHLs against tree contact, exploiting line design standards and publicly available datasets to characterize an analytical model of the physical interaction between lines and environment. The model accounts for the specific geometric, mechanical and electrical features of the lines as well as for the specific features of the environment (e.g. forecasted weather conditions, terrain slope, characteristics of the tree species, etc.). Simulations demonstrate that the proposed model can identify the MV grid areas critical for tree fall, as confirmed by the resilience plan of the DSO, and that under severe weather conditions, also HV lines may be affected by faults induced by tree falls. Results show how to characterize the OHL vulnerability, its dependence on specific trimming or ROW maintenance policies and on weather forecasts, also catching the criticality due to the simultaneity of snow and wind loads. The analytical model also assures lower sensitivity to classification errors with respect to the vulnerability models derived from failure statistics.

Acknowledgment

This work has been financed by the Research Fund for the Italian Electrical System in compliance with the Decree of Minister of Economic Development April 16, 2018.

The authors also gratefully acknowledge the contributions of Deval.

References

[1] K. Finch e C. Allen, "Understanding Tree Caused Outages", in EEI Natural Resource Conference, Palm Springs, CA, April 2001.

[2] M. Panteli, P. Mancarella, "Influence of extreme weather and climate change on the resilience of power systems: Impacts and possible mitigation strategies", *El. Power Systems Research*, Elsevier, 2015.

[3] S. Guggenmoos, "Outage Statistics - As a Basis for Determining Line Clearance Program Status," *UAA Quarterly*, 1996.

[4] CORINE database. Available at: https://land.copernicus.eu/pan-european/corine-land-cover/

[5] T. Todic, P.C. Chen, M. Kezunovic, "Risk Analysis for Assessment of Vegetation Impact on Outages in Electric Power Systems", CIGRE US National Committee Symposium, 2016.

[6] E. Ciapessoni, D. Cirio, G. Kjølle, S. Massucco, A. Pitto e M. Sforna, "Probabilistic risk based security assessment of power systems considering incumbent threats and uncertainties," *Special issue on "Power System Resilience" of IEEE Transactions on Smart Grid,* vol. 7, n. 6, pp. 2890-2903, Nov. 2016.

[7] IEEE Std 738, "IEEE Standard for Calculating the Current-Temperature of Bare Overhead Conductors," January 2007.

[8] C. Alegria, M. Tomé, "A tree distance-dependent growth and yield model for naturally regenerated pure uneven-aged maritime pine stands in central inland of Portugal", *Annals of Forest Science*, *Springer Verlag/EDP Sciences*, Vol. 70, No. 3, pp.261-276, 2013.

[9] H. Peltola, S. Kellomäki, "A mechanistic model for calculating windthrow and stem breakage of Scots pines at stand edge", *Silva Fenn*. Vol 27, pp. 99–111, 1993.

[10] K. Kamimura, K. Kitagawa, S. Saito, H. Mizunaga "Root anchorage of hinoki (Chamaecyparis obtusa (Sieb. Et Zucc.) Endl.) under the combined loading of wind and rapidly supplied water on soil: analyses based on tree-pulling experiments", *European Journal of Forest Research* vol. 131, pp. 219-227, 2012.

[11] P. G. Blackwell, K. Rennolls, M. P. Coutts, "A root anchorage model for shallowly rooted Sitka spruce". *Forestry*, Vol 63, pp. 73-91, 1990.

[12] R. Coutts, "Components of tree stability in Sitka spruce on peaty gley soil", *Forestry*, Vol 59, Issue 2, pp. 173-197, 1986.

[13] B. Gardiner H. Peltola S. Kellomaki "Comparison of two models for predicting the critical wind speeds required to damage coniferous trees", *Ecological Modelling* , vol. 129, pp. 1-23, 2000.

[14] M. Shibuya, A. Koizumi, H. Torita, "Tree shape and resistance to uprooting – a simple model analysis", *Eurasian J For Res* , Vol. 17, issue 1, pp. 11-17, 2014.

[15] A. Achim, B. Nicoll, S. Shaun, B. Gardiner, "Wind stability of trees on slopes", *Proc. of Int. Conf Wind effects on trees*, Karlsruhe, Germany, Sept 2003.

[16] CENELEC Std. EN 50341-2-13:2017-01, "Overhead electrical lines exceeding AC 1 kV - Part 2-13: National Normative Aspects (NNA) for Italy (based on EN50341-1:2012).

[17] CEI (Italian Electrotechnical Committee) Std 11-4, "Norme tecniche per la costruzione di linee elettriche aeree esterne", (in Italian), 1998-9.

[18] Deval, 2015, "Progetto Smart Grid - Cabina Primaria di Villeneuve", final report (in Italian).

[19] Regione Val d'Aosta, 2018, "Geographic Information System (GIS),". Available: http://geonavsct.partout.it/pub/GEoCartoSCT/ .

[20] A. Guarneri and M. Forteleoni, "Caratteristiche generali delle linee elettriche aeree facenti parte della RTN", TERNA, 2011 (in Italian).

[21] AEP (American Electric Power) Ohio, "Encroachments on Transmission Rights of Way", technical paper, 2015.

[22] DEVAL, "Resilience Plan 2019-2021", Addendum to development plan 2019-2021, Dec 2018 (in Italian).